Demixing of Hydrogen and Helium at Megabar Pressures

Winfried Lorenzen, Bastian Holst, and Ronald Redmer
Institut für Physik, Universität Rostock, D-18051 Rostock, Germany
(Received 6 October 2008; published 16 March 2009)

We present results of *ab initio* finite-temperature density functional theory molecular dynamics simulations for fluid hydrogen-helium mixtures at megabar pressures. The location of the miscibility gap is derived from the equation of state data. We find a close relation between hydrogen-helium phase separation and the continuous nonmetal-to-metal transition in hydrogen. Our calculations predict that demixing of hydrogen and helium occurs in Saturn and probably also in Jupiter. These results will have a strong impact on interior models of giant solar and extrasolar planets.

DOI: 10.1103/PhysRevLett.102.115701 PACS numbers: 61.20.Ja, 31.15.A−, 64.30.−t, 71.30.+h

Giant planets such as Jupiter and Saturn consist mostly of hydrogen and helium along with a small amount of heavier elements. The basic input into the respective interior models is an accurate equation of state (EOS) for the hydrogen-helium mixture at high pressures. Demixing into a helium-rich and a helium-poor phase would explain the lower helium content in Jupiter's [1,2], and probably also Saturn's, outer region and the high luminosity of Saturn, which exceeds the theoretical value based on homogeneous interior models by about 50%.

The progress in shock wave experimental techniques has allowed us to probe pressures of a few Mbar in hydrogen [3] and helium [4]. States deep in the interior reach still higher pressures up to 45 Mbar in the core of Jupiter and 10 Mbar in Saturn, which up to now have only been treated by theoretical methods. The EOS of hydrogen-helium mixtures is usually calculated by a linear mixing (LM) of the individual equations of state. First detailed studies of the properties of hydrogen-helium mixtures and of a possible phase separation have been performed, e.g., by Stevenson [5] using fluid perturbation theory and later by Hubbard and DeWitt [6] who applied Monte Carlo simulations for a fully ionized H-He plasma. The low-pressure regime was studied by Schouten *et al.* [7] by a Monte Carlo technique using effective pair potentials for the atoms and molecules in the mixture.

Only a few attempts have been made so far to calculate the EOS of H-He mixtures from first-principles. Klepeis *et al.* [8] performed total energy calculations for *solid* H-He alloys based on the local density approximation of density functional theory (LDA-DFT). They found an almost pressure-independent demixing temperature of 15 000 K for a He fraction of $x = N_{\mathrm{He}}/(N_{\mathrm{He}} + N_{\mathrm{H}}) = 0.07$ as relevant for Jupiter and Saturn, implying that demixing is relevant for both planets. However, thermal effects were considered only by combining the $T = 0$ K electronic structure calculations with the ideal entropy of mixing.

Pfaffenzeller *et al.* [9] applied *ab initio* Car-Parrinello molecular dynamics (CP-MD) simulations in the pressure range $4\ \mathrm{Mbar} \leq P \leq 24\ \mathrm{Mbar}$ at temperatures $T \leq 3000$ K to calculate the excess Gibbs free energy of mixing. They also combined their low-temperature electronic structure calculations within the LDA-DFT for the liquid mixture with the ideal entropy of mixing and derived much lower demixing temperatures. For instance, for a 10% He fraction they found demixing already below 7000 K at 10 Mbar so that it might occur in Saturn but definitely not in Jupiter, contrary to the former result. These CP-MD simulations were only performed up to 3000 K and include the correlations in the liquid. Higher temperatures were considered in the ideal entropy only. Note that these *ab initio* results [8,9] predict layer boundaries which do not agree with current planetary models [10–13].

Vorberger *et al.* [14] performed first-principles DFT-MD simulations by using the generalized gradient expansion (GGA) instead of the LDA for fluid hydrogen-helium mixtures with a mixing ratio of $x = 0.333$ and $x = 0.075$ in order to evaluate the accuracy of the LM approximation. They found deviations of up to 8% in energy and volume at constant pressure for temperatures $500 \leq T \leq 8000$ K and densities $0.19 \leq \varrho \leq 0.66\ \mathrm{g/cm^3}$, which underlines the necessity to go beyond the LM approximation for planetary conditions.

An adequate quantum statistical treatment of phase separation in hydrogen-helium mixtures has to consider correlations *as well as* thermal excitations in the warm, high-pressure fluid. Therefore, we have performed extensive finite-temperature (FT-)DFT-MD simulations employing a Fermi occupation of the electronic states using Mermin's approach [15], which is implemented in the plane wave density functional code VASP [16,17]. We consider 32 to 128 atoms in the simulation box and periodic boundary conditions. The electron wave functions are calculated using the projector augmented wave (PAW) potentials [18,19] supplied by VASP with PAW cutoffs of $r_{\mathrm{cut}} = 0.52$ Å which are sufficiently small compared to the interatomic distances. As in [14] we use GGA in the parametrization of Perdew, Burke, and Ernzerhof [20]. We have chosen a plane wave cutoff E_{cut} at 1200 eV such that the pressure is converged within 1% accuracy. We have also checked the convergence with respect to a systematic enlargement of the **k**-point set in the representation of the Brillouin zone. Higher-order **k**-points modify the EOS data only within 1% relative to a one-point result so that we have restricted our EOS calculations to the Baldereschi mean value point [21]. The simulations were performed for a canonical ensemble with temperature, volume of the simulation box, and particle number therein as given quantities. The ion temperature was controlled by a Nosé-Hoover thermostat. After 1000 time steps of 0.2 to 1.0 fs the system was equilibrated and the subsequent 2000 to 5000 steps were taken to calculate the EOS data.

The dynamic conductivity $\sigma(\omega)$ was derived from the Kubo-Greenwood formula [22,23]; for a numerical evaluation; see Refs. [24–26]. We have used various **k**-point sets for the integration of the Brillouin zone to ensure that the conductivity was converged better than 20% over the entire density range.

Demixing occurs whenever the Gibbs free energy $G(x)$ of the system can be minimized by separating into two phases with different values of x. Since $G(x)$ is not directly accessible within the simulations we have first calculated the enthalpy of mixing

$$\Delta H(x) = H(x) - xH(1) - (1-x)H(0), \tag{1}$$

for up to 33 different values of x by evaluating the enthalpy $H(x)$ in terms of internal energy $U(x)$, pressure P, and volume $V(x)$ via $H(x) = U(x) + PV(x)$ at constant temperatures and pressures. The results are fitted by using a Redlich-Kister expansion [27]

$$\Delta H_{\mathrm{RK}}(x) = (x^2 - x)\sum_{i=1}^{n} A_i (2x-1)^{i-1}. \tag{2}$$

To reproduce the calculated enthalpy of mixing by better than 5%, an expansion up to fifth order ($n = 5$) is necessary. We add the ideal entropy of mixing as in [8,9]

$$\Delta S_{\mathrm{id}}(x) = -k_B[x\ln x + (1-x)\ln(1-x)], \tag{3}$$

where k_B is the Boltzmann constant, to obtain the Gibbs free energy of mixing

$$\Delta G(x) = \Delta H_{\mathrm{RK}}(x) - T\Delta S_{\mathrm{id}}(x) \tag{4}$$

for a given temperature and pressure. The neglect of the nonideal entropy of mixing is an open approximation which has, up to now, unknown effects on the thermodynamic results. The major improvement with respect to earlier works is the correct treatment of thermal effects in $\Delta H(x)$ which are treated more consistently in our Born-Oppenheimer MD than in CP-MD.

We have evaluated the Gibbs free energy of mixing (4) for several temperatures up to 20 000 K at three different pressures $P = 4$, 10, and 24 Mbar as in [9] and constructed the miscibility gap for these conditions which are relevant for the interiors of Jupiter and Saturn. We show the Gibbs free energy of mixing as a function of the helium fraction for different temperatures at a constant pressure of 4 Mbar in Fig. 1. For temperatures below 11 000 K a region with negative curvature exists which leads to phase separation. The behavior for low temperatures (e.g., 2000 K) changes and is more complex due to the formation of solid He, which is discussed later (see Figs. 2 and 3). For higher temperatures the (ideal) entropy of mixing ensures positive curvature and, thus, the H-He system is always miscibile. This typical behavior is found for all pressures considered here.

A common double tangent construction is applied to identify the phase separation region. The resulting demixing temperatures are shown in Fig. 2 as a function of the helium fraction x. Although the EOS data have an accuracy of better than 2%, we estimate the error for the demixing temperatures to be less than 10% for $x \leq 0.5$ and better than 20% for $x > 0.5$, respectively, due to the sensitivity of the double tangent construction to errors in $\Delta G(x)$. Our *ab initio* results reveal a surprising and unexpected behavior of hydrogen-helium mixtures at high pressures. For low helium fractions $x \leq 0.3$ we obtain only a weak pressure dependence in contrast to the former CP-MD simulations [9]. Furthermore, the miscibility gap is strongly asymmetric which is also reflected by the need for higher-order Redlich-Kister expansions (2) in order to ensure the required accuracy of the EOS data. For all considered pressures a kink appears in the helium-rich region at about $x \approx 0.7$–0.9 which deserves closer attention. The demixing temperature has a finite value for the very helium-rich part and then rises sharply at a certain pressure-dependent hydrogen fraction. This behavior can only be understood by studying the complex interplay between the thermodynamic instability and the electronic transition that occur at such high pressures.

We discuss first the finite demixing temperatures for nearly pure helium. These values can clearly be identified

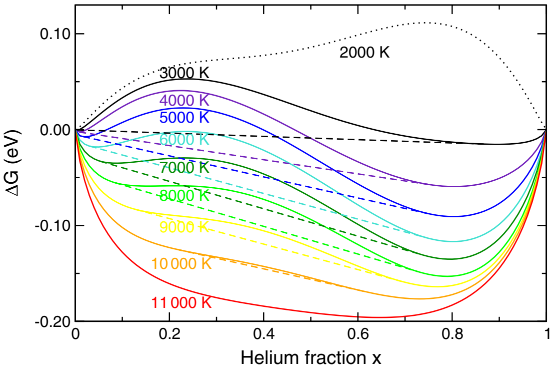

FIG. 1 (color online). Gibbs free energy of mixing for a pressure of 4 Mbar. For temperatures below 11 000 K a region with negative curvature occurs for which the common double tangent construction is applied (dashed lines).

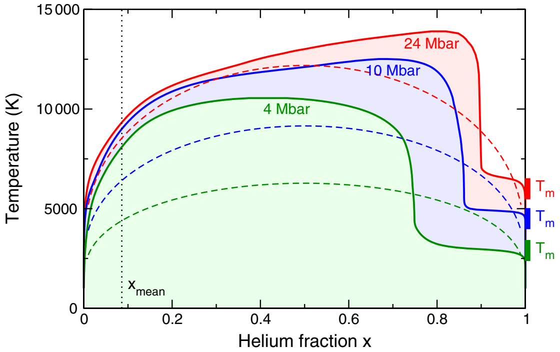

FIG. 2 (color online). Miscibility gap in the hydrogen-helium system for three pressures. Our results (solid lines) show a strongly asymmetric slope in contrast to CP-MD results [9] (dashed lines). The dotted line represents the mean helium fraction in Jupiter. The calculated melting temperatures T_m of solid helium are indicated on the right side for each pressure.

with the melting temperature T_m of the helium solid at the respective pressure, indicated by the colored vertical bars on the right side of Fig. 2. We have determined the high-pressure phase diagram of helium in more detail by analyzing the pair correlation functions and the ionic diffusion coefficient. Calculations for the internal energy along isochores have shown that jumps of about 0.2–0.36 eV per He atom occur due to melting. We have added our new high-pressure EOS data to the helium phase diagram given by Loubeyre *et al.* [28] and Datchi *et al.* [29] in Fig. 3. The melting line resulting from our simulations agrees well with the extrapolation of the measured high-pressure melting line, except that our data indicate a slight curvature.

The second, even more astonishing feature of the miscibility gap shown in Fig. 2 is the abrupt increase of the demixing temperature. This occurs at hydrogen fractions which obey the relation $n_H^{1/3} a_B \approx 0.25$ for each pressure. We have calculated the electrical conductivity of the hydrogen-helium mixture by evaluating the Kubo-Greenwood formula [22–25] and can derive three main results: (i) pure helium is nonmetallic for all pressures and temperatures considered here with conductivities reaching $\sigma_{\mathrm{He}} \geq 10^4/\Omega$ m only at temperatures higher than $T = 15\,000$ K at 24 Mbar; (ii) the conductivity is about $\sigma \approx 5 \times 10^3/\Omega$ m at $n_H^{1/3} a_B \approx 0.25$ which corresponds to the minimum metallic conductivities reported for doped semiconductors such as In:CdS and P:Si [30]; (iii) we reproduce the measured electrical conductivity and the measured value of $n_H^{1/3} a_B \approx 0.38$ for metallization [3] in pure hydrogen fluid (i.e. at $x = 0$), see Ref. [25]. Therefore, it is now obvious that the thermodynamics which drives the phase separation in hydrogen-helium mixtures is caused by a continuous nonmetal-to-metal transition in the hydrogen subsystem. Metallic hydrogen and nonmetallic helium demix up to high temperatures unless the ideal entropy of mixing favors a mixed state again.

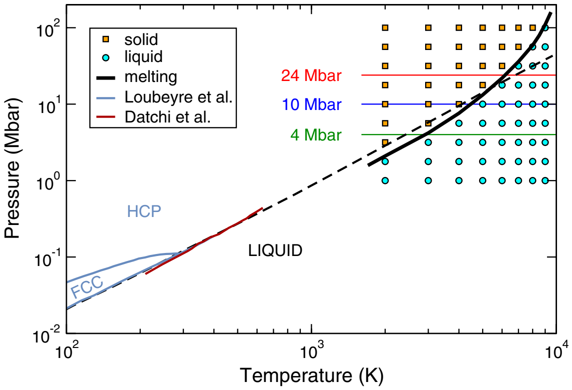

FIG. 3 (color online). Melting line and phase diagram of helium. Our results (colored points) agree well with the extrapolation (dashed line) of the measurements by Loubeyre *et al.* [28] and Datchi *et al.* [29]. The three isobares considered are also shown. Note that the temperatures inside the planets are higher than those on the melting line so that no solid helium occurs there.

The great impact of our new results for the phase separation of hydrogen and helium on interior models of Jupiter and Saturn is illustrated in Fig. 4. We compare the demixing temperatures as function of the pressure at the mean helium fraction $x = 0.086$ with the corresponding isentropic P-T relations in both planets, taken from [11]. To evaluate the behavior also at pressures below 4 Mbar we have calculated additional points at 1 and 2 Mbar by considering only few relevant temperatures, without identifying the whole miscibility gap. The uncertainties of these points are, therefore, slightly higher than for the other pressures. We have included the result of Schouten *et al.* [7] which should be valid at low pressures in the molecular fluid.

For pressures between 1–2.6 Mbar, i.e., from $0.86R_J$ to $0.76R_J$, the temperature in Jupiter is likely to be below the demixing temperature so that phase separation should occur. For pressures above $P_T = 2.6$ Mbar, hydrogen and helium are miscible again. This corresponds well with a

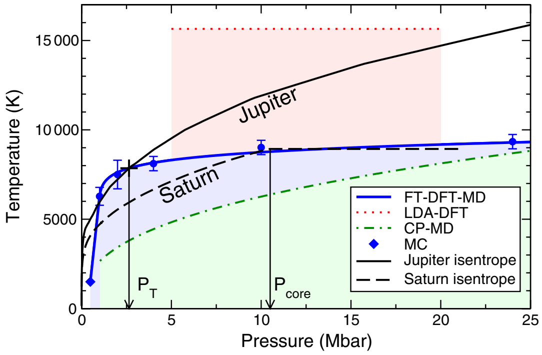

FIG. 4 (color online). Region of demixing in the P-T plane and isentropes for Jupiter and Saturn. Our new FT-DFT-MD results (with error bars) in combination with the low-pressure result of Schouten *et al.* [7] are compared with the LDA-DFT calculations [8] for a solid H-He alloy and the CP-MD curve [9].

transition pressure of about 4 Mbar as derived from the most recent Jupiter model of Nettelmann *et al.* [11] who have processed an almost complete set of FT-DFT-MD EOS data for the individual planetary materials H, He (the same as used here for $x = 0$ and $x = 1$), and H_2O. They applied the LM approximation to construct a new Jupiter model assuming the standard three-layer structure.

The most striking result of our simulations is that the temperature of Saturn above 0.8 Mbar (i.e., below 0.68 R_S) is almost completely below the demixing temperature except a very small region at the core (indicated by P_{core}). Such a phase separation has first been proposed by Stevenson and Salpeter [31,32] in order to explain the high luminosity of Saturn and its age. This has prompted further detailed studies. For instance, Fortney and Hubbard [12] could reproduce the correct age of Saturn only by assuming complete phase separation of hydrogen and helium which is now confirmed by our results. According to the usual assumption we expect that a helium-rich phase is located above the core which is continuously accumulated by helium droplets raining down due to gravity, and that the remaining fluid envelope is slowly depleted.

In conclusion, we have performed consistent *ab initio* FT-DFT-MD simulations for the phase diagram of hydrogen-helium mixtures at high pressures as relevant for planetary interiors. We obtain only a weak pressure dependence of the demixing temperature for low helium fractions but a strongly asymmetric demixing curve with respect to the helium fraction x. We find that pure helium ($x = 1$) is in the solid phase for pressures of several Mbar, and only the fluid phase at higher temperatures is miscible with nonmetallic hydrogen. The demixing temperature strongly increases at hydrogen fractions of $n_H^{1/3} a_B \approx 0.25$, where the hydrogen component undergoes a nonmetal-to-metal transition and demixing from insulating helium occurs.

Our results are of particular importance for interior models of giant planets. Hydrogen-helium demixing in Jupiter is likely to occur in a small region between 1–2.6 Mbar, i.e., just at the boundary between the two fluid envelopes of usual three-layer models. While the outer envelope demixes partially and a depleted helium amount follows, the layer below is a miscible hydrogen-helium fluid with a higher helium fraction than average. The interior of Saturn is in the phase separation region above 0.8 Mbar which gives strong arguments that hydrogen-helium demixing—as long has been predicted—is responsible for the high luminosity of that planet. If our results lead to four-layer models with a helium gradient or three-layer models persist due to convection remains to be studied by advanced planetary models.

We thank Nadine Nettelmann, Martin French, André Kietzmann, Thomas R. Mattsson, Peter Hauschildt, and Ralf Neuhäuser for helpful discussions. This work was supported by the Deutsche Forschungsgemeinschaft within the SFB 652 and the project RE 882/11, and the Supercomputing Center North (HLRN).

[1] J. N. Bahcall, M. H. Pinsonneault, and G. J. Wasserburg, Rev. Mod. Phys. **67**, 781 (1995).
[2] U. von Zahn, D. M. Hunten, and G. Lehmacher, J. Geophys. Res. **103**, 22 815 (1998).
[3] S. T. Weir, A. C. Mitchell, and W. J. Nellis, Phys. Rev. Lett. **76**, 1860 (1996).
[4] V. Y. Ternovoi, S. V. Kvitov, A. A. Pyalling, A. S. Filimonov, and V. E. Fortov, JETP Lett. **79**, 6 (2004).
[5] D. J. Stevenson, Phys. Rev. B **12**, 3999 (1975).
[6] W. B. Hubbard and H. E. DeWitt, Astrophys. J. **290**, 388 (1985).
[7] J. A. Schouten, A. de Kuijper, and J. P. J. Michels, Phys. Rev. B **44**, 6630 (1991).
[8] J. E. Klepeis, K. J. Schafer, T. W. Barbee III, and M. Ross, Science **254**, 986 (1991).
[9] O. Pfaffenzeller, D. Hohl, and P. Ballone, Phys. Rev. Lett. **74**, 2599 (1995).
[10] T. Guillot, Science **286**, 72 (1999).
[11] N. Nettelmann, B. Holst, A. Kietzmann, M. French, and R. Redmer, Astrophys. J. **683**, 1217 (2008).
[12] J. J. Fortney and W. B. Hubbard, Icarus **164**, 228 (2003).
[13] J. J. Fortney and W. B. Hubbard, Astrophys. J. **608**, 1039 (2004).
[14] J. Vorberger, I. Tamblyn, B. Militzer, and S. A. Bonev, Phys. Rev. B **75**, 024206 (2007).
[15] N. D. Mermin, Phys. Rev. **137**, A1441 (1965).
[16] G. Kresse and J. Hafner, Phys. Rev. B **47**, 558 (1993).
[17] G. Kresse and J. Furthmüller, Phys. Rev. B **54**, 11 169 (1996).
[18] P. E. Blöchl, Phys. Rev. B **50**, 17 953 (1994).
[19] G. Kresse and D. Joubert, Phys. Rev. B **59**, 1758 (1999).
[20] J. P. Perdew, K. Burke, and M. Ernzerhof, Phys. Rev. Lett. **77**, 3865 (1996).
[21] A. Baldereschi, Phys. Rev. B **7**, 5212 (1973).
[22] R. Kubo, J. Phys. Soc. Jpn. **12**, 570 (1957).
[23] D. A. Greenwood, Proc. Phys. Soc. London **71**, 585 (1958).
[24] M. P. Desjarlais, J. D. Kress, and L. A. Collins, Phys. Rev. E **66**, 025401 (2002).
[25] B. Holst, R. Redmer, and M. P. Desjarlais, Phys. Rev. B **77**, 184201 (2008).
[26] A. Kietzmann, B. Holst, R. Redmer, M. P. Desjarlais, and T. R. Mattsson, Phys. Rev. Lett. **98**, 190602 (2007).
[27] O. Redlich and A. T. Kister, Ind. Eng. Chem. **40**, 345 (1948).
[28] P. Loubeyre, R. LeToullec, J. P. Pinceaux, H. K. Mao, J. Hu, and R. J. Hemley, Phys. Rev. Lett. **71**, 2272 (1993).
[29] F. Datchi, P. Loubeyre, and R. LeToullec, Phys. Rev. B **61**, 6535 (2000).
[30] P. P. Edwards, R. L. Johnston, C. N. R. Rao, D. P. Tunstall, and F. Hensel, Phil. Trans. R. Soc. A **356**, 5 (1998).
[31] D. J. Stevenson and E. B. Salpeter, Astrophys. J. Suppl. Ser. **35**, 221 (1977).
[32] D. J. Stevenson and E. B. Salpeter, Astrophys. J. Suppl. Ser. **35**, 239 (1977).